DOI: https://doi.org/10.15407/pmach2025.04.026

UDC 539.3

STRENGTH ASSESSMENT OF THE GAS TURBINE ENGINE FAN DISK BASED ON ITS FRACTURE TOUGHNESS ANALYSIS

Pavlo P. Hontarovskyi, gontarpp@gmail.com
ORCID: 0000-0002-8503-0959

Serhii V. Ugrimov, sugrimov@ipmach.kharkov.ua
ORCID: 0000-0002-0846-4067

Natalia V. Smetankina, nsmetankina@ukr.net
ORCID: 0000-0001-9528-3741

Nataliia H. Garmash, garm.nataly@gmail.com
ORCID: 0000-0002-4890-8152

Iryna I. Melezhyk, melezhyk81@gmail.com
ORCID: 0000-0002-8968-5581

Tetiana V. Protasova, tatyprotasova@gmail.com,
ORCID: 0000-0003-1489-2081

Anatolii Pidhornyi Institute
of Power Machines and Systems
of NAS of Ukraine,
2/10, Komunalnykiv str., Kharkiv, 61046, Ukraine

The competitiveness and economic efficiency of aviation gas turbine engines (GTE) are determined by the level of their reliability and resource. One of the most stressed elements of the GTE are disks. It is known that their destruction can lead to an air crash, and structural, technological, operational and other factors can be the cause of this. The specified level of reliability must be ensured throughout the entire engine operation. The evaluation of the crack resistance of the GTE fan disk using an improved method for calculating the development of cracks in structures under cyclic loading, which is based on determining the magnitude of elastic-plastic deformations by the finite element method in the area of the crack tip, is given in the paper. The study was performed for two options of the calculation scheme. In the first one, the disk is considered taking into account the interlocking joints of the blade shanks, which are in contact with the disk teeth. They are modeled by a layer with orthotropic material properties. For the second option of the calculation scheme, the interlocking joints were not included in the model, and the load was applied to the disk rim. In this case, the centrifugal force load from the interlocking joint was taken into account. It was established that the hub of the disk is more stressed than the rim. The nature of the destruction of the GTE disk from the hub and rim sides is different, which is explained by the change in circumferential stresses in the direction of the crack depth. The crack displacement during the destruction of the disk in the rim occurs in the radial direction, and in the hub – in the axial direction. The results of the conducted research will increase the period of reliable operation of aircrafts, reduce the costs and time of their development, and will also contribute to increasing safety in performing civil and combat missions.

Keywords: *crack resistance, stress-strain state, finite element method, strength, reliability.*

Introduction

Due to the fact that gas turbine engines provide high efficiency, reliability and power in a wide range of operating conditions, they are considered key elements of modern aviation and power engineering. One of their most important components is the fan disks, which operate under conditions of significant mechanical loads and cyclic operating modes. A necessary condition for the reliability and stable operation of the engine as a whole is to ensure their strength and durability under difficult operating conditions.

The growing requirements for the economy, environmental friendliness and resource of gas turbine units require new approaches to the design, modeling and assessment of the disks strength. Scientists [1, 2] pay special attention to the analysis of the stress-strain state, the influence of geometric parameters, materials and manufacturing technologies on the operational characteristics, as well as the development of means of improvement [3] and increase of the reliability of the gas turbine engine (GTE). One of the most threatening defects affecting the safety of operation and requiring comprehensive research are cracks, the change in size of which during rotation, as well as the variable contact of their edges, lead to destruction and the occurrence of emergency situations. That is why a significant number of scientific papers are devoted to the analysis of the processes of crack formation and distribution [4, 5].

In this paper, the strength of fan disks of gas turbine engines is assessed based on the analysis of their crack resistance taking into account modern operating conditions, and recommendations are given to increase their service life and reliability.

Problem statement

Using an improved method for assessing the stress-strain state and crack resistance of structural elements [6, 7], the strength of a D-18T type gas turbine engine fan [8] made of VT3-1 titanium alloy was assessed.

The physical properties of the titanium alloy [9] are given below: density ρ=4.5 g/cm^3; modulus of elasticity E=1.15×10^5 MPa; Poisson's ratio ν=0.3. The coefficients of Hooke's law for an isotropic elastic material through physical constants are determined by the formulas

$$A_{11}=\frac{E\cdot(1-\nu)}{(1+\nu)\cdot(1-2\nu)}=154808 \text{ MPa};\quad A_{12}=\frac{E\cdot\nu}{(1+\nu)\cdot(1-2\nu)}=66346 \text{ MPa};\quad A_{44}=\frac{E}{2\cdot(1+\nu)}=45100 \text{ MPa}.$$

The GTE fan has 33 blades with fir-tree shanks with three teeth. The length of the blade airfoil is about 86.2 cm, the length of the shank is 3.5 cm.

To determine the stress-strain state of the disk, we will consider two options of the calculation scheme. In the first of them, the disk is considered taking into account the layer of the interlocking joints. The interlocking joints of the blade shanks that contact the disk teeth are modeled by a layer with orthotropic material properties. Centrifugal forces from the blade airfoil P_b are transmitted to the shanks, which, in turn, through contact interactions with the disk teeth (Fig. 1) load the disk rim together with the centrifugal forces of the shanks and disk teeth.

The forces from the blade airfoil, which act on the orthotropic layer of the interlocking joints, are distributed evenly over a cylindrical surface with a radius of r_b=0.385 m and a generating length of l=0.25 m, whose area is $2\pi\cdot0.385\cdot0.25$=0.60476 m^2. The centrifugal force of the blade airfoil is taken to be 1.8326 MN. Thus, the radial stresses σ_r on the layer of interlocking joints from the blade airfoil of 33 blades are

$$\sigma_r=\frac{1.8326\cdot33}{2\pi\cdot0.385\cdot0.25}=100 \text{ MPa}.$$

The gaps between the teeth of the shanks and the disk can be neglected, therefore the specific gravity of the orthotropic layer of the interlocking joints is taken to be the same as that of the disk material (titanium alloy VT3-1).

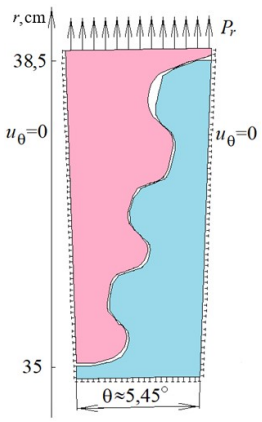

Fig. 1. Scheme of fir-tree interlocking joint of blades with disk

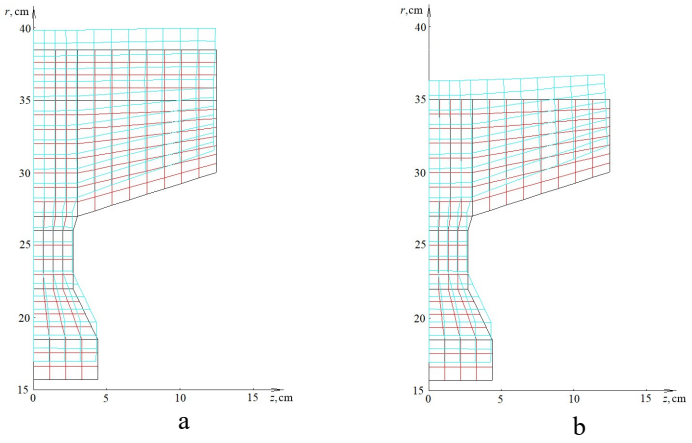

Fig. 2. Meridional section of the disk with finite element discretization:
a – first option of the calculation scheme;
b – second option of the calculation scheme

Elastic properties of the orthotropic layer of the interlocking joints in the radial r and axial z directions of A_{11} and A_{22} are taken to be approximately two times smaller compared to the VT3-1 material, since the area of the teeth of the shank and the disk is almost the same. In the circumferential direction, the layer of the interlocking joints is loaded insignificantly. For these reasons, the elastic orthotropic properties of the interlocking joints are taken as follows: A_{11}=80000 MPa; A_{12}=3000 MPa; A_{44}=4000 MPa; A_{22}=70000 MPa; A_{33}=1000 MPa; A_{13}=A_{23}=100 MPa.

A meridional section of the disk with finite element discretization, as well as a deformed state of the disk, where the displacements are increased by 10 times, is shown in Fig. 2.

For the second option of the calculation scheme, we do not take into account the interlocking joints, and the load is applied to the disk rim at a radius of r=0.35 m. In this case, the centrifugal force load from the interlocking joint of 27.5 MPa is added to the load from the blades. The disk rotation speed is 628 rad/s=6000 rpm. Thus, the radial load at a radius of r=0.35 m will be equal to 137 MPa. The first option of the calculation scheme is more accurate, since additional bending stiffness in the meridional plane of the disk rim teeth is taken into account.

The aim of the study is to assess the crack resistance of the disk in the presence of an axial scratch between two adjacent teeth with a depth of 0.15 cm and a length of 9.5 cm under zero cyclic loading, which corresponds to the period from takeoff to landing of the aircraft.

The radial-axial crack in the disk rim develops according to the fatigue brittle fracture diagram using the stress intensity coefficient at the vertices (marked "+" and "-") of the semi-elliptical surface crack (Fig. 3). The stress intensity coefficient at the maximum load in the cycle is determined by the method of Ovchinnikov A. V. [10].

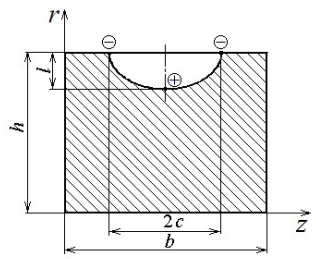

Fig. 3. Cross-section of a body in the plane of a semi-elliptical crack

Calculation of crack resistance of the GTE disk

To calculate the kinetics of a radial-axial crack in the rim of a gas turbine engine disk, we first determine the stress-strain state of the disk in an axisymmetric formulation [6, 7] for both options of the calculation schemes using the finite element method in order to compare the results.

The distribution of radial σ_r, axial σ_z and circumferential σ_θ stresses, as well as the stress intensity σ_i for the first option of the calculation scheme are shown in Figs. 4–7.

To calculate the stress intensity factor K_I according to the method of Ovchinnikov A. V. [10], the region of the disk rim in the form of a rectangle measuring 8 cm×25 cm is considered. In this case, the change in stresses σ_θ is taken into account only in the radial direction. Since in reality they also change in the axial direction, we will consider the stresses along the median plane of the disk, as well as on the fifth row of finite elements at z=0.3594 cm (Fig. 2), which will take into account the average value of $\sigma_\theta(r)$.

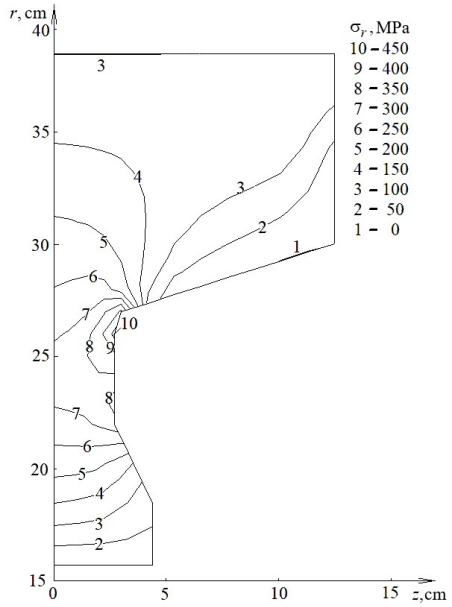

Fig. 4. Distribution of radial stresses σ_r for the first option of the calculation scheme

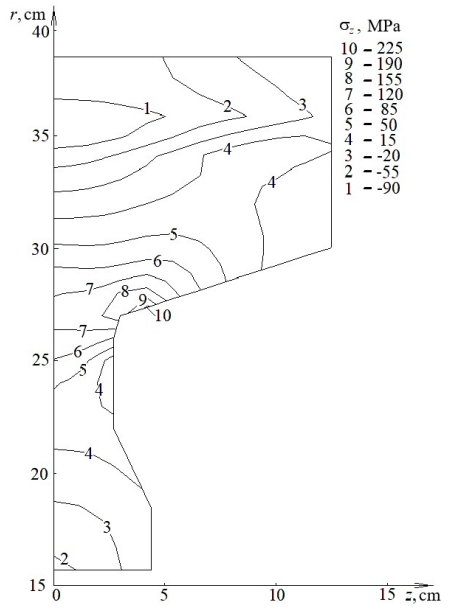

Fig. 5. Distribution of axial stresses σ_z for the first option of the calculation scheme

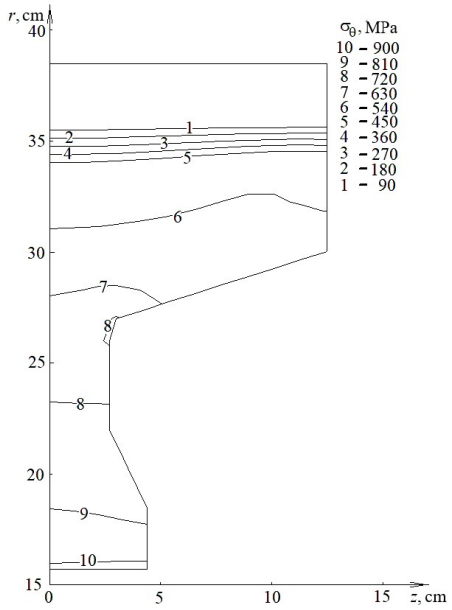

Fig. 6. Distribution of circumferential stresses σ_θ for the first option of the calculation scheme

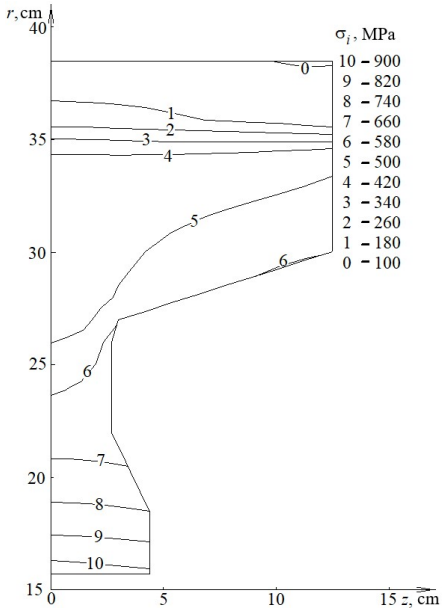

Fig. 7. Stress intensity distribution σ_i for the first option of the calculation scheme

Table 1. Stresses $\sigma_\theta(x)$ in the rim of the disk

σ_r, MPa	z, sm	x, sm								
		0	0.5	1.5	2.5	3.5	4.5	5.5	6.5	7.5
		σ_θ, MPa								
100	0	434.00	447.3	473.8	500.2	527.4	556.0	586.5	618.0	647.9
	3.594	457.05	467.6	488.7	510.4	533.1	557.5	584.9	616.5	672.1
137	0	365.75	385.2	424.1	462.8	501.6	541.3	581.8	621.3	656.2
	3.594	401.90	418.4	451.4	485.1	519.7	556.1	595.9	640.5	715.9

The values of stresses $\sigma_\theta(r)$ for calculating the kinetics of cracks in the disk rim are given in Table 1, where x=38.5 cm – r cm.

The rate of development of a surface semi-elliptical crack $\frac{dl}{dN}$ under cyclic loading in the VT3-1 material is described by the Paris equation [6, 7]

$$\frac{dl}{dN} = 2 \cdot 10^{-10} \cdot K_{\mathrm{I}}^{2,2},$$

where K_{I} – stress intensity coefficient at the crack tip, MPa √m; N – number of load cycles.

When the stress intensity factor reaches the level $K_{\mathrm{I}}=K_{1C}$=250 MPa √m the disk will be fractured (downwards).

Results of calculations of the disk crack resistance at the initial parameters of a semi-elliptical crack l_0=0.15 cm, c_0=9.5 cm are given in Table 2.

In the table, $l_{\max}$, $c_{\max}$ are the crack resistance parameters at the moment of disk failure; $N_{\max}$ is the number of load cycles at the moment of disk failure; K_I^+, K_I^- are the values of the stress intensity coefficients at the moment of failure at points "+" and "-", respectively (Fig. 3), in which the maximum crack sizes $l_{\max}$, $c_{\max}$ are determined. The results for σ_r=100 MPa z=3.594 cm can be considered more accurate because they take into account the bending stiffness of the interlocking joints and the averaged circumferential stresses over the width of the rim.

The obtained circumferential stresses in the median plane of the disk are underestimated due to the significant flexibility of the rim in the rz plane; therefore, they give overestimated values of the number of cycles to failure.

The disk hub is more stressed than the rim. For this hub, calculations of the kinetics of a crack that developed from the groove in the form of a semi-elliptical crack with semi-axes l_0=0.1 cm, c_0=0.5 cm from the inner cylindrical surface were performed.

The material properties and the kinetic diagram were taken to be the same as for the disk rim. The circumferential stresses were averaged over the thickness of the hub. Their values for both options of the calculation scheme are given in Table 3.

Table 2. Crack resistance parameters of the disc rim at the time of fracture

σ_r, MPa	z, sm	l_{max}, sm	c_{max}, sm	N_{max}, cycles	K_I^+, MPa√m	K_I^-, MPa√m
100	0	3.85	10.4	7580	250	180
	3.594	3.75	10.3	6800	250	180
137	0	4.20	10.4	10800	250	178
	3.594	4.00	10.4	8860	250	178

Table 3. Values of circumferential stresses σ_θ in the disk hub

σ_r, MPa	x, sm							
	0	0.4667	1.4000	2.3333	3.2375	4.1125	4.9875	5.8625
	σ_θ, MPa							
100	915.45	894.0	851.1	815.3	787.5	768.4	755.2	743.9
137	919.25	897.7	854.6	818.7	790.7	771.5	758.3	746.9

Table 4. Parameters of the crack resistance of the hub of the disk at the time of failure

σ_r, MPa	l_{max}, sm	c_{max}, sm	N_{max}, cycles	K_I^+, MPa√m	K_I^-, MPa√m
100	1.725	2.464	2826	202	250
137	1.720	2.360	2800	202	250

The results of calculations of the kinetics of a semi-elliptical crack in the hub of the disk are given in Table 4. Fig. 8 shows the dependence of the crack depth l on the number of cycles to failure N: the dotted line indicates the result for the first option of the calculation scheme; the solid line indicates the result for the second option of the calculation scheme.

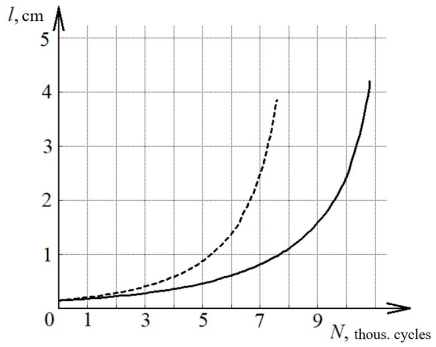

Fig. 8. Dependence of the crack depth l in the disk rim on the number of cycles N
(the dotted line indicates the result for the first calculation scheme, the solid line indicates the result for the second one)

It should be noted that in the disk hub for both calculation schemes, similar results were obtained both in terms of the values of the circumferential stresses and in terms of the number of cycles to failure. In the process of crack growth to a depth of x, the stresses σ_θ in the rim increased, and in the hub – decreased. The destruction of the disk in the rim occurred at the point l_{max}, while in the hub – at the point c_{max}.

Since there are no reliable data on the disk blading, calculation studies were carried out for cases when the value of the centrifugal force from the blades airfoil is 10% less and 10% more than the accepted one. In this case, the load from the blade tip on the cylindrical surface at r=38.5 cm cannot exceed 110 MPa, since with a higher load, plastic deformations will occur in the hub. Calculations were made for the load options σ_r=90 MPa and σ_r=110 MPa at a radius of 38.5 cm, as well as for σ_r=126 MPa and σ_r=146 MPa at a radius of 35 cm without interlocking joints.

Table 5. Stress values $\sigma_\theta(x)$ in the rim

σ_r, MPa	z, sm	x, sm								
		0	0.5	1.5	2.5	3.5	4.5	5.5	6.5	7.5
		σ_θ, MPa								
90	0	406.30	418.8	443.8	408.6	494.6	521.0	549.6	579.2	607.3
	3.594	427.80	437.7	457.6	478.6	499.3	522.3	548.0	577.6	629.6
110	0	461.65	475.7	503.8	531.9	560.7	591.1	623.4	656.9	688.6
	3.594	486.35	497.5	519.8	542.7	566.8	592.7	621.8	655.4	714.7
126	0	343.20	361.5	398.1	434.3	470.8	508.0	545.9	583.0	615.7
	3.594	377.00	392.5	423.5	455.0	487.5	521.7	558.9	600.8	671.2
146	0	338.10	408.8	450.2	491.2	532.5	574.7	617.7	659.6	696.6
	3.594	426.75	444.3	479.0	515.1	551.9	590.6	632.8	680.3	760.6

The obtained stress values $\sigma_\theta(x)$ for calculating the kinetics of cracks in the rim are given in Table 5.

The results of calculations of the crack resistance of the disk rim at values of centrifugal forces of blading, lower and higher than those accepted, are given in Table 6.

The values of circumferential stresses $\sigma_\theta(x)$ in the disk hub at values of centrifugal forces of blading, lower and higher than those accepted, for both options of the calculation schemes are given in Table 7.

The results of calculations of the crack resistance of the disk hub at values of centrifugal forces of blading lower and higher than those accepted are given in Table 8.

Calculated crack resistance studies for centrifugal force values 10% lower and 10% higher than the accepted one showed that the number of cycles to failure increases and decreases by approximately 15%, respectively.

Table 6. Parameters of crack resistance of the disk rim at the moment of fracture at different levels of centrifugal forces of blading

σ_r, MPa	z, sm	l_{max}, sm	c_{max}, sm	N_{max}, cycles	K_I^+, MPa√m	K_I^-, MPa√m
90	0	4.10	10.5	8840	250	186
	3.594	4.02	10.5	7960	250	190
110	0	3.61	10.2	6540	250	174
	3.594	3.50	10.2	5860	250	174
126	0	4.43	10.6	12540	250	183
	3.594	4.23	10.5	10320	250	184
146	0	3.98	10.4	9420	250	174
	3.594	3.77	10.3	7700	250	174

Table 7. Values of circumferential stresses $\sigma_\theta(x)$ in the disk hub at different values of centrifugal forces of blading for both options of the calculation schemes

r, sm	σ_r, MPa	x, sm							
		0	0.4667	1.4000	2.3333	3.2375	4.1125	4.9875	5.8625
		σ_θ, MPa							
38.5	90	860.1	839.9	799.5	765.8	739.6	721.5	708.9	698.1
	110	970.8	948.1	851.1	815.3	787.5	768.4	755.2	743.9
35.0	126	864.6	844.3	854.6	769.9	743.5	725.3	712.7	701.9
	146	973.8	951.0	90.4	867.5	838.0	817.7	803.8	792.0

Table 8. Parameters of crack resistance of the disk hub at the moment of fracture at different levels of centrifugal forces of blading

σ_r, MPa	l_{max}, sm	c_{max}, sm	N_{max}, cycles	K_I^+, MPa√m	K_I^-, MPa√m
90	1.79	2.46	3280	201	250
110	1.66	2.27	2440	204	250
126	1.78	2.45	3200	200	250
146	1.66	2.26	2420	204	250

Conclusions

When studying the crack resistance of the GTE fan disk, two options of calculation schemes were considered with different nature of taking into account the transfer of forces from the blade airfoil tip to the disk. In the first scheme, the transfer of forces is modeled by a layer taking into account the interlocking joints, in the second one, the interlocking joints are not taken into account, and the loads are evenly distributed over the disk rim.

When studying the crack resistance of the GTE fan disk, two options of calculation schemes were considered: when the radial load of the blade separation is evenly distributed over the cylindrical surface at r=38.5 cm and without taking into account the interlocking joints, the load is applied at r=35 cm.

The results obtained in the calculations taking into account the interlocking joints at the averaged stresses σ_θ over the width of the rim should be considered more accurate, since in this case, in the rz plane, the bending stiffness of the teeth of the interlocking joints is included in the total stiffness.

Significant refinements of the results when calculating the crack resistance of the disk rim allow to obtain the averaging of the circumferential stresses over the width of the rim. In the hub, the occurrence of even minor surface defects in the form of scratches or dents is dangerous.

The nature of the failure of the GTE disk from the hub and rim sides is different, which is explained by the change in the circumferential stresses in the direction of the crack depth. The crack displacement during the failure of the disk in the rim occurs in the radial direction, and in the hub – in the axial direction.

Computational studies of the crack kinetics were carried out for cases when the value of the centrifugal force from the blade airfoil is 10% less and 10% more than the accepted one. The results showed that the number of cycles to failure changes by approximately 15% (increases in the first case and decreases in the second one).

Analysis of the crack resistance of fan disks of gas turbine engines for various loading cases proved that the presence and development of a crack significantly affects the number of cycles to failure, therefore, to ensure reliable operation and timely detection of cracks, it is necessary to conduct inter-repair inspections in the rim at least every 1 thousand, and in the hub – after 2 thousand flight cycles.

Financing

The results of this article were partially obtained as part of the research work on the Target Scientific and Technical Program of Defense Research of the National Academy of Sciences of Ukraine for 2025–2029, program expenditure classification code 6541230 (applied research).

References

1. Masiahin, V. I., Hryhorenko, A. M., Konokh, K. M., & Khakhalkina, O. A. (2021). *Vyznachennia faktoriv, yaki znyzhuiut pokaznyky nadiinosti dyskiv HTD ta rozrobka zakhodiv po yikh pidvyshchenniu* [Determination of factors that reduce the reliability of GTE disks and development of measures to increase them]. *Systemy upravlinnia, navihatsii ta zviazku – Control, Navigation and Communication Systems*, vol. 3, no. 65, pp. 50–55 (in Ukrainian). https://doi.org/10.26906/SUNZ.2021.3.050.
2. Tovkach, S. (2025). *Adaptyvni kinematychni struktury do pobudovy konstruktsii aviatsiinoho hazoturbinnoho dvyhuna* [Adaptive kinematic structures for building an aircraft gas turbine engine design]. *Aviatsiino-kosmichna tekhnika i tekhnolohiia – Aerospace Technic and Technology*, no. 4 sup 1, pp. 157–162 (in Ukrainian). https://doi.org/10.32620/aktt.2025.4sup1.20.
3. Kvasha, Yu. O. & Zinevych, N. A. (2021). *Aerodynamichne vdoskonalennia ventyliatora aviatsiinoho hazoturbinnoho dvyhuna* [Aerodynamic improvement of the fan of an aircraft gas turbine engine]. *Tekhnichna mekhanika – Technical Mechanics*, no. 3, pp. 23–29 (in Ukrainian). https://doi.org/10.15407/itm2021.03.023.
4. Orenes Moreno, B., Bessone, A., Solazzi, S., Vanti, F., Bagnera, F., Riva, A., & Botto, D. (2022). Linear elastic fracture mechanics assessment of a gas turbine vane. *Materials*, vol. 15, iss. 13, article 4694. https://doi.org/10.3390/ma15134694.
5. Leonel, E. D. & Venturini, W. S. (2011). Probabilistic fatigue crack growth using BEM and reliability algorithms. *Boundary Elements and Other Mesh Reduction Methods XXXIII*, vol. 52, pp. 3–14. https://doi.org/10.2495/BE110011.
6. Hontarovskyi, P. P., Smetankina, N. V., Garmash, N. H., & Melezhyk, I. I. (2020). Analysis of crack growth in the wall of an electrolyser compartment. *Journal of Mechanical Engineering – Problemy mashynobuduvannia*, vol. 23, no. 4, pp. 38–44. https://doi.org/10.15407/pmach2020.04.038.
7. Hontarovsky, P. P., Smetankina, N. V., Ugrimov, S. V., Harmash, N. H., & Melezhyk, I. I. (2022). Simulation of the crack resistance of ion-exchange strengthened silicate glass subject to bending strain. *International Applied Mechanics*, vol. 58, iss. 6, pp. 715–724. https://doi.org/10.1007/s10778-023-01195-0.
8. (2025). Turbofan Aircraft engines D-18T, Series 3. JSC "Motor Sich": official website. https://motorsich.com/ukr/products/aircraft/tde/d-18t/.
9. Characteristics for grade VT3-1. Database of Steel and Alloy [electronic resource]. https://www.splav-kharkov.com/main.php.
10. Shulzhenko, M. H., Hontarovskyi, P. P., Matiukhin, Yu. I., Melezhyk, I. I., & Pozhydaiev, O. V. (2011). *Vyznachennia rozrakhunkovoho resursu ta otsinka zhyvuchosti rotoriv i korpusnykh detalei turbin* [Determination of estimated resource and evaluation of rotor life and body parts of turbines]: Methodological guidelines. Regulatory document SOU-N MEV 0.1–21677681–52:2011: approved by the Ministry of Energy and Coal Mining of Ukraine: effective as of 07.07.11. Kyiv: Ministry of Energy and Coal Mining of Ukraine, 42 p. (in Ukrainian).

Received 22 November 2025
Accepted 12 December 2025

Оцінка міцності диска вентилятора газотурбінного двигуна на основі аналізу його тріщиностійкості

П. П. Гонтаровський, С. В. Угрімов, Н. В. Сметанкіна, Н. Г. Гармаш, І. І. Мележик, Т. В. Протасова

Інститут енергетичних машин і систем ім. А. М. Підгорного НАН України,
61046, Україна, м. Харків, вул. Комунальників, 2/10

Конкурентоспроможність й економічна ефективність авіаційних газотурбінних двигунів (ГТД) визначаються рівнем їх надійності й ресурсу. Одними із найбільш напружених елементів ГТД є диски. Відомо, що їх руйнування може привести до авіакатастрофи, а причинами цього можуть бути конструктивні, технологічні, експлуатаційні та інші фактори. Заданий рівень надійності повинен забезпечуватися впродовж всього часу експлуатації двигуна. У роботі проведено оцінку тріщиностійкості диска вентилятора ГТД за допомогою удосконаленої методики розрахунку розвитку тріщин у конструкціях при циклічному навантаженні, яка ґрунтується на визначенні розмахів пружно-пластичних деформацій методом скінченних елементів у районі вершини тріщини. Дослідження виконано для двох варіантів розрахункової схеми. У першому з них диск розглядається із урахуванням замкових з'єднань хвостовиків лопаток, які контактують із зубцями диска. Вони моделюються шаром із ортотропними властивостями матеріалу. Для другого варіанта розрахункової схеми замкові з'єднання не включалися до моделі, а навантаження прикладалося до обода диска. При цьому бралося до уваги навантаження відцентрових сил від замкового з'єднання. Установлено, що ступиця диска більш напружена, ніж обід. Характер руйнування диска ГТД зі сторони ступиці і обода різний, що пояснюється зміною окружних напружень у напрямку глибини тріщини. Зрушення тріщини під час руйнування диска в ободі відбувається в радіальному напрямку, а у ступиці – в осьовому. Результати проведених досліджень дозволять підвищити строк надійної експлуатації літальних апаратів, зменшити витрати і час їх розробки, а також сприятимуть підвищенню безпеки при виконанні цивільних і бойових завдань.

***Ключові слова**: тріщиностійкість, напружено-деформований стан, метод скінченних елементів, міцність, надійність.*

Література

1. Масягін В. І., Григоренко А. М., Конох К. М., Хахалкіна О. А. Визначення факторів, які знижують показники надійності дисків ГТД та розробка заходів по їх підвищенню. *Системи управління, навігації та зв'язку*. 2021. Т. 3. № 65. С. 50–55. https://doi.org/10.26906/SUNZ.2021.3.050.
2. Товкач С. Адаптивні кінематичні структури до побудови конструкції авіаційного газотурбінного двигуна. *Авіаційно-космічна техніка і технологія*. 2025. № 4 sup 1. С. 157–162. https://doi.org/10.32620/aktt.2025.4sup1.20.
3. Кваша Ю. О., Зіневич Н. А. Аеродинамічне вдосконалення вентилятора авіаційного газотурбінного двигуна. *Технічна механіка*. 2021. № 3. С. 23–29. https://doi.org/10.15407/itm2021.03.023.
4. Orenes Moreno B., Bessone A., Solazzi S., Vanti F., Bagnera F., Riva A., Botto D. Linear elastic fracture mechanics assessment of a gas turbine vane. *Materials*. 2022. Vol. 15. Iss. 13. Article 4694. https://doi.org/10.3390/ma15134694.
5. Leonel E. D., Venturini W. S. Probabilistic fatigue crack growth using BEM and reliability algorithms. *Boundary Elements and Other Mesh Reduction Methods XXXIII*. 2011. Vol. 52. P. 3–14. https://doi.org/10.2495/BE110011.
6. Hontarovskyi P. P., Smetankina N. V., Garmash N. H., Melezhyk I. I. Analysis of crack growth in the wall of an electrolyser compartment. *Journal of Mechanical Engineering – Problemy mashynobuduvannia*. 2020. Vol. 23. No. 4. P. 38–44. https://doi.org/10.15407/pmach2020.04.038.
7. Hontarovsky P. P., Smetankina N. V., Ugrimov S. V., Harmash N. H., Melezhyk I. I. Simulation of the crack resistance of ion-exchange strengthened silicate glass subject to bending strain. *International Applied Mechanics*. 2022. Vol. 58. Iss. 6. P. 715–724. https://doi.org/10.1007/s10778-023-01195-0.
8. Турбореактивний двоконтурний авіаційний двигун Д-18Т серії 3. АТ «Мотор Січ»: офіційний сайт. 2025. https://motorsich.com/ukr/products/aircraft/tde/d-18t/.
9. Характеристика материала ВТ3-1. Марочник стали и сплавов [электронный ресурс]. https://www.splav-kharkov.com/main.php.
10. Визначення розрахункового ресурсу та оцінка живучості роторів і корпусних деталей турбін. Методичні вказівки: СОУ- Н МЕВ 40.1–21677681– 52:2011 / М. Г. Шульженко, П. П. Гонтаровський, Ю. І. Матюхін, І. І. Мележик, О. В. Пожидаєв. Київ: ОЕП «ГРІФРЕ»: М-во енергетики та вугільної пром-сті України, 2011. 42 с.